International Journal on Emerging Technologies 13(1): 56-64(2022)

ISSN No. (Print): 0975-8364
ISSN No. (Online): 2249-3255

Linear-Quadratic Regulator-based SSR Mitigation Scheme for SSSC Controller in DFIG-based SERIES Compensated Network

Chirag Rohit[1], Pranav B. Darji[2] and Hitesh R. Jariwala[2]
[1]Research Scholar, Department of Electrical Engineering,
Sardar Vallabhbhai National Institute of Technology, Surat (Gujarat), India.
[2]Associate Professor,Department of Electrical Engineering,
Sardar Vallabhbhai National Institute of Technology, Surat (Gujarat), India.

(Corresponding author: Chirag Rohit)
(Received 05 April 2022, Revised 06 May 2022, Accepted 20 May 2022)
(Published by Research Trend, Website: www.researchtrend.net)

ABSTRACT: A wind turbine generator based long transmission network with series capacitance may suffer sub-synchronous oscillations at low wind speed and high compensation. This paper presents an enhancement of sub-synchronous resonance (SSR) stability caused due to extensive series compensation of transmission line using linear quadratic regulation (LQR) based approach for a static synchronous series capacitor (SSSC) in Doubly Fed Induction Generator (DFIG). An extensive use of series compensation even at light wind can cause the prone conditions for invoking SSR in windfarms. Among all the signals of the network, the electromagnetic torque produced by DFIG reflects SSR instability predominantly. Hence the torque signal of DFIG is modulated and voltage injected by SSSC is regulated to dampen the SSR oscillations in the torque signal using the LQR approach. For modulating the torque signal, the actuating efforts are varied by SSSC. The impact of LQR based damping approach for improvement in SSR mode at high compensation levels and low wind speed is examined using eigen value analysis and time domain simulations. The proposed method can effectively improve SSR stability even at low wind speeds and high compensation levels.

Keywords: Damping Controller, Linear quadratic regulation, sub-synchronous resonance, wind farms.
Abbreviations: SSR, Sub Synchronous Resonance; SSSC, Static Synchronous Series Compensator; FSC, Fixed Series Capacitor; DFIG, Doubly Fed Induction Generator; RSC, Rotor Side Converter; GSC, Grid Side Converter, IGE Induction Generation Effect; LQR Linear Quadratic Regulator

I. INTRODUCTION

The share of green energy in the global power sector is increasing rapidly. Wind energy is one of the most widely utilized green energy resources. Modern wind turbines are categorized into three categories based on their location and how they connect to the grid: Land-based (onshore) wind farms, offshore windfarms, and distributed wind farms. The nameplate capacity of land-based windfarms averages 250MW, whereas distributed wind farms have a capacity of up to50 kW [1]. The offshore wind farms are bulk in size, more vigorous, and produce more power than land-based wind farms. Its capacity range begins at 200 kW and continues to grow significantly [2]. According to the list of biggest off shore wind farms presently under construction, the lowest capacity is 400MW, and the maximum is 8200 MW [1, 3, 4]. One of the most prevalent barriers to wind energy integration into the grid is the need for a new transmission line to connect wind farms with high-load locations. Moreover, as the transmission length increases, the losses related to power transmission and inductive reactance of the transmission line increase [5]. As a result, it becomes difficult to transfer immense power to a large load. In such cases, fixed series capacitors placed in the transmission line directly oppose the inductive reactance of the transmission line, thus reducing the transmission line's length virtually [6, 7]. This approach is inexpensive, and it makes a voltage level through the transmission line constant and therefore improves the system's performance [8]. However, the adverse phenomenon called sub-synchronous resonance (SSR) can arise due to the large-scale integration of induction generator-based wind farms with series compensated transmission lines. According to the survey of different types of wind power generators connected with series compensated transmission lines, the severity of SSR is high in doubly-fed induction generators (DFIG) [9–12]. Thus, the DFIG-based power network needs a suitable controller to operate the system stably and securely.

Various approaches are proposed in the literature to show the effectiveness of damping SSR oscillations [13–15]. The mitigation through grid side converter (GSC) and rotor side converter (RSC) is an economical solution because they have in-built converter control capabilities. GSC has less potentiality over SSR damping because the GSC power rating is only 25% to 30% of DFIG's rating [16–18]. While the RSC converter has a higher rating than the GSC converter and directly controls the active and reactive power produced by the DFIG [19]. As a result, oscillations caused primarily by sub-synchronous control interactions (SSCI) are effectively dampened [20, 21]. But SSR produced due to other effects is less mitigated because increasing the RSC control gain reduces aggregated transmission line

impedance resistance, which may cause the induction generation effect type SSR [22, 23]. The effectiveness of static varcompensator (SVC) for SSR mitigation in a series-compensated wind farm is explored in literature [24, 25]. This approach is often applied due to the benefits of reactive power support and its ease of implementation. In a DFIG-based wind farm, the impedance control technique at a fixed firing angle using thyristor-controlled series capacitor (TCSC) provides damping to SSCI owing to RSC [26]. The gate-controlled series capacitor (GCSC) may also be used to reduce SSR in DFIG-based wind farms; it utilizes power scheduling controller (PSC) to regulate reactance in order to maintain the transmission line's power flow [27, 28]. Utilizing TCSC or GCSC can minimize sub-synchronous oscillations in DFIG-based wind farms and dampen unstable SSR mode, but it may also affect super synchronous mode stability [29]. The above literature remarks that an additional damping scheme is needed with FACTS device to enhance the mitigation to SSR mode without affecting other modes. Conversely, the use of a linear quadratic regulator-based SSR mitigation scheme with a FACTS device to mitigate SSR in DFIG-based wind farms is obscure. Thus, this paper shows the application of the Linear quadratic regulation (LQR) approach with SSSC to demonstrate SSR characteristics.

SSSC is an advanced type of controlled series compensating device. SSSC injects reactive voltage in the transmission line in quadrature with line current in order to regulate power flow. For enhancing SSR stability an LQR-based damping approach can be applied with SSSC, which can dampen the oscillation produced due to SSR by controlling the voltage injected by SSSC. LQR is a state-feedback controller that applies a state-space system form for optimally designing and controlling the system [30]. The values of the state-feedback gain matrix can be achieved using the pole placement method. In this report, the SSR characteristics of the study system with SSSC and the proposed damping controller scheme are shown by performing eigenvalue analysis and transient simulation. The major objective of this paper is to demonstrate the effect of SSSC with LQR for SSR alleviation at low wind speed and high compensation levels. The results show that the LQR improves the stability of SSR significantly.

The organization of this paper is as follows. Section 2 presents introduction of the study system and mathematical model of SSSC. Section 3 Analysis of SSR in DFIG-based wind farms at different passive compensation levels and shows a comparison of important results through eigenvalue analysis along with the design of the proposed LQR control scheme is presented, and Section4 involves eigenvalue analysis and time domain response after including SSSRDC in the study system.

II. STUDY SYSTEM

The study system for the DFIG-based series capacitive compensated transmission line is remodeled using IEEE first benchmark model (FBM) for SSR studies [22]. It consists of a 161-kV series compensated transmission line interfaced with a 100 MW wind farm and infinite grid, as shown in Fig. 1. It is reasonable to add fixed series compensation since the transmission line is around 154 miles in length to increase its power transfer capability. The wind farm is made up of 50 units of 2 MW wind turbine generating units. For stability analysis of the study system, the small-signal models for each subsystem, such as shaft system, IG, back-to-back converters, and transmission line, are described in the next subsections, and their parameters are listed in the Appendix.

The complete differential equations-based model of the study system and modal analysis of system modes for the SSR study has been presented in the authors' previous research [31]. Hence, this paper omitted a detailed discussion on differential equations and impacting parameters. The focus will be on the application of the LQR approach with SSSC in a phased manner using the controllability index for enhancing SSR mode stability in DFIG-based series compensated network. In summary, a 4th order model is used to describe the dynamics of an induction generator's stator and rotor currents in the synchronous reference frame. As the induction generator (IG) is developed in the synchronous reference frame, the series compensated transmission network is also developed in the same reference frame for easy mathematical analysis. A two-mass model is used to relate the dynamics of the IG-turbine drive train system. The IG is equipped with back-to-back controllers with dc link capacitor. The dynamic of the dc-link capacitor placed between the RSC and the GSC is contemplated by a first-order differential equation using active power balance consideration. The RSC and GSC inside loops are current govern loops, and the outside loops are the power/voltage govern loops. In RSC control, the q-axis loop and d-axis loops track the active and reactive power references, respectively, as shown in Fig. 2. While through the GSC control, the q-axis loop and d-axis loop track the dc-link reference voltage and DFIG terminal voltage, respectively, as shown in Fig. 3.

Additionally, SSSC is utilized in transmission lines along with a fixed series capacitor (FSC) to increase stability and power transfer through the line. The transmission line's series compensation is split into FSC and SSSC at a 2:1 ratio to improve stability at the transmission line's peak compensation level. This paper proposes the application of LQR control to SSSC to further improve the SSR mode stability by steering the transmission line model's states to stable surfaces. Hence subsequent subsection shows the analysis of SSR under various critical conditions such as peak compensation levels and light wind.

Study System and Stability Assessment. This subsection presents SSR analysis of the study system with passive compensation in the transmission line exclusively. Due to the insertion of FSC in the transmission line, the line current carries two frequency components f_n and f_e, where f_e is a fundamental frequency, and f_n is a natural frequency according to the compensation level. The natural frequency f_n can be estimated by

$$f_n = f_e \sqrt{\frac{X_c}{X_{Total}}}. \quad (1)$$

Where Xc is the series capacitive reactance of the FSC placed in the transmission line, and X_{Total} is the aggregate sum of inductive reactance of the study

system submodules as a transmission line (X_L), transformer (X_T), and system (X_{sys}). The induction generation effect fundamentally provokes in the induction generator due to slip s_1 defined as,

$$s_1 = \frac{f_n - f_r}{f_n} \tag{2}$$

where f_r is electrical frequency in Hz based on IG rotor speed.

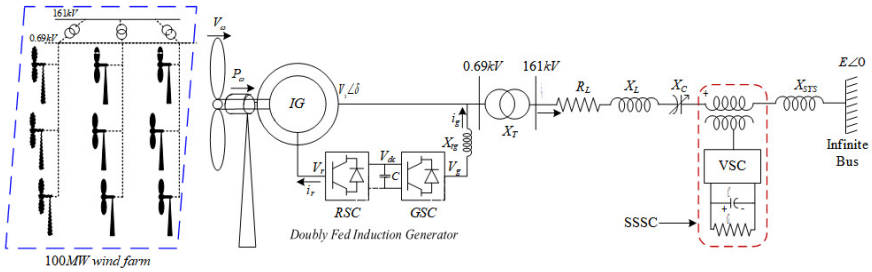

Fig. 1. Study System with SSSC.

The dissimilitude among series-capacitive compensation level of the transmission line and wind speed may adversely affect the stability of DFIG-based transmission system due to the induction generation effect in the DFIG. In normal operation, If the wind turbine is rotating at the rated speed and the transmission line is series-compensated, then f_r will be higher than the natural Frequency (f_n). In such conditions, the smaller magnitude of s_1 with a negative sign can make the rotor resistance R_r higher than the network and DFIG stator winding resistance (R_s + R_L). Such incidents may provoke the risk of IGE-type SSR in DFIG-based wind farms. The small-signal analysis is accomplished using the differential equations of subparts of the study system shown [40] to analyze the SSR stability of the study system considering the variation of wind speed and compensation level. Table 1 shows the list of eigenvalues for discrete compensation levels at unvarying wind speeds, while Table 2 shows the list of eigenvalues for different wind speeds at fixed compensation levels.

From Table 1 and Table 2, it is seen that Mode-2 is unstable when the compensation level is greater than 50%, and the wind speed is less than 8 m/s. Mode-2 can be associated with SSR phenomena because the shaft of the turbine-generator model experiences two frequencies (f_n and f_e) when FSC is placed in the transmission line. As the compensation level of FSC is increased, the SSR mode leads to instability because slip s_1 is negative with less value. Due to this R_r is greater than (R_s + R_L) which produces induction generator effect type SSR in DFIG. The next section provides a step-by-step mathematical representation for SSSC with a controller to eliminate SSR.

Modeling of Static Synchronous Series Compensator. This sub-section presents the mathematical modeling of SSSC in the qd reference frame to improve the SSR characteristics of the system by injecting a reactive voltage into the transmission line. The schematic diagram of SSSC with the study system is shown in Fig. 1. SSSC improves the power flow through the transmission line and stability of the study system by injecting the voltage.

The injection of SSSC voltage in RL transmission network in qd reference frame can be shown as,

$$\frac{d}{dt}\begin{bmatrix} i_{ql} \\ i_{dl} \end{bmatrix} = \begin{bmatrix} -\frac{\omega_b}{X_L}R_L & -\omega_e \\ \omega_e & -\frac{\omega_b}{X_L}R_L \end{bmatrix}\begin{bmatrix} i_{ql} \\ i_{dl} \end{bmatrix} + \frac{\omega_b}{X_L}\begin{bmatrix} v_{qs} - v_{qC} - E_q \\ v_{ds} - v_{dC} - E_d \end{bmatrix}. \tag{3}$$

Where R_L and X_L are resistance and inductive-reactance of the transmission line respectively; E is the voltage of the infinite grid, v_t is the DFIG's terminal voltage, i_l is the transmission line current and v_{sC} is the voltage injected by SSSC.

The v_{qsC} and v_{dsC} are active and reactive components of the SSSC voltage v_{sC}.

Table 1: List of modes for varying compensation level at fixed wind speed.

Comp. level	Mode 1	Mode 2	Mode 3	Mode 4
15%	-6.6168±489.9i	-5.3671±263.35i	-3.815±93.982i	-0.4939±6.1474i
25%	-7.1122±522.75i	-5.1904±230.08i	-4.1877±93.956i	-0.49368±6.1476i
50%	-8.3147±582.99i	-3.8851±168.88i	-5.8905±93.811i	-0.49285±6.1483i
75%	-9.5903±629.17i	1.6034±123.7i	-11.602±91.825i	-0.49119±6.1496i
90%	-10.42±653.25i	6.3734±108.15i	-16.399±82.919i	-0.48923±6.1509i

Table 2: List of modes for varying wind speed at a fixed compensation level.

Wind speed	Mode 1	Mode 2	Mode 3	Mode 4
7 m/s	-9.5903±629.17i	1.6034±123.7i	-11.602±91.825i	-0.49119±6.1496i
8 m/s	-9.4742±629.14i	-3.0053±121.9i	-7.1014±55.389i	-0.47438±6.1557i
9 m/s	-9.4227±629.14i	-4.4819±121.73i	-86.199±38.091i	-0.32311±6.1673i
10 m/s	-9.3961±629.13i	-5.1831±121.68i	-86.597±37.942i	-0.56888±6.2055i

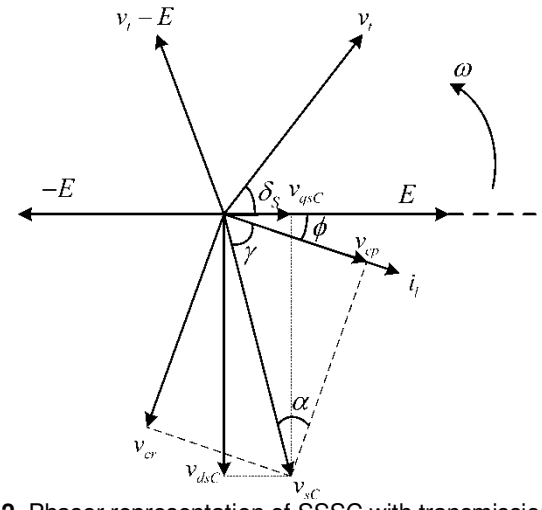

Fig. 2. Phasor representation of SSSC with transmission line.

Fig. 2 shows the insertion of SSSC voltage in the transmission line system through a phasor diagram. The active component and reactive component of v_{sC} can be further expressed as

$$v_{qC} - jv_{dC} = (v_{cp} - jv_{cr})e^{-j\phi} = v_{sC}e^{-j(\gamma+\phi)} \quad (4)$$

Eventually, SSSC voltage v_{sC} makes the phase angle (γ+Ø). In (5), γ is an angle by v_{sC} lags line current i_l. The v_{cp} is in phase with i_l, and vcr is in quadrature withil. They can be further expressed as $v_{cp} = v_{sC}(\cos(\gamma))$ and $v_{cr} = v_{sC}(\sin(\gamma))$. Ø is phase-angle of line current il which is defined as

$$\tan\phi = -\frac{i_{ql}}{i_{dl}} \quad (5)$$

In this paper, v_{cr} is considered as positive if v_{sC} lags line current il. It signifies that if v_{cr} leads il then the working mode of SSSC is inductive, and if v_{cr} lags il then the working mode is capacitive. Here v_{cp} is negligible due to a very small loss in DC capacitor of VSC. That will only be conceivable if γ is close to 90◦. It can be expressed mathematically as

$$\gamma = sgn(V_{cr})\left[-\frac{pi}{2} + \alpha\right] \quad (6)$$

The dynamic response of DC capacitor of VSC is expressed as

$$\frac{d}{dt}v_{sdc} = -\frac{G}{C}v_{sdc} + \frac{i_{sdc}}{C}. \quad (7)$$

Where v_{sdc} is the voltage applied across the DC link capacitor of the VSC; G and C, respectively, are its conductance and capacitance. Using a power balance estimation in steady state operation, the power on the DC side of VSC is considered the same as the active power on the AC side of VSC. Hence,

$$v_{sdc}i_{sdc} = Re(v_{sC}i_l^*) = v_{cp}i_l = kv_{sdc}i_l \sin\alpha. \quad (8)$$

In this approach, to stabilize the network, the ratio of the ac voltage output of SSSC to DC voltage across VSC in SSSC (k = v_{sC}/v_{sdc}) is held constant, and its value is held $2\sqrt{6}/\pi$ by assuming 12-pulse VSC is used for SSSC. The angle α is controlled. In Fig. 2, the active and reactive voltage added by SSSC is defined by considering in-phase and quadrature elements of v_{sC}.

LQR Control Approach.

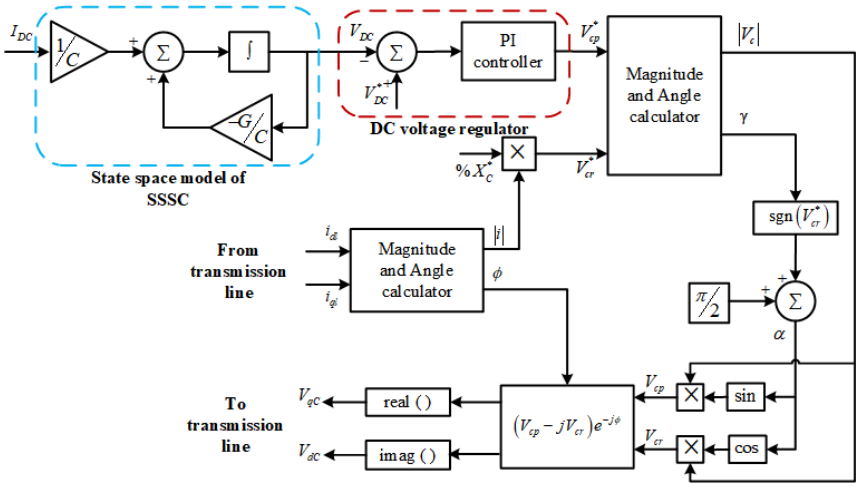

Fig. 3. Schematic representation of SSSC with transmission line current.

The LQR is an optimal control approach for multi-input and higher-order system [32], where the optimal performance of the system can be achieved by the proper chosen of the state-feedback gain matrix (K). The values of K are determined depending on the desired location of poles using the pole placement method. Given amulti-input linear system

$$\dot{x} = Ax + Bu \tag{9}$$

The optimal pole location can be defined by the LQR depending on the cost function. The optimal solution is determined using the control input (u), which is used to minimize the quadratic cost function (J)

$$\mathrm{J} = \int_0^\infty (x^T Q x + u^T R u) dt \tag{10}$$

where Q is coefficient of convergence rate and rate is coefficient of cost $Q \geq 0$ and $R > 0$ are symmetric, positive (semi-) definite matrices of the appropriate dimension. This cost function represents a balance between the distance of the state from the origin and the cost of the control input. By choosing the matrices Q and R, described in more detail below, we can balance the rate of convergence of the solutions with the cost of the control.

The solution to the LQR problem is given by a linear control law of the form

$$u = -R^{-1} B^T P x \tag{11}$$

Where P is a positive definite, symmetric matrix that satisfies the equation

$$PA + A^T P - PBR^{-1} B^T P + Q = 0. \tag{12}$$

Eqn. (13) is known as the algebraic Riccati equation and can be solved numerically by using the "*lqr*" command in MATLAB.

For the minimization of the cost function the weights Q and R should be chosen by studying the behavior of the system which is to be controlled. A particular combination of diagonal weights for Q and R, are found as

$$Q = \begin{Bmatrix} q_1 & 0 & \cdots \\ 0 & \ddots & 0 \\ \vdots & 0 & q_n \end{Bmatrix} \tag{13}$$

$$R = \rho \begin{Bmatrix} r_1 & 0 & \cdots \\ 0 & \ddots & 0 \\ \vdots & 0 & r_n \end{Bmatrix} \tag{14}$$

For this choice of Q and R, the individual diagonal elements describe how much each state and input (squared) should contribute to the overall cost.

LQR is used for dampening of SSR oscillations to improve stability by regulating the oscillatory signal in literature [33, 34]. In this paper, LQR is used for the enhancement of SSR mode and is connected with the SSSC controller. Since SSSC injects the reactive voltage to regulate the power flow and improve the system stability, the LQR used in this paper uses voltage injected by SSSC in order to minimize the error of electromagnetic torque of DFIG. Since the torque produced by DFIG reflects SSR instability in the best way, the error between reference torque value and actual torque is chosen as a quadratic performance index (J), which will be regulated by SSSC voltage. The electromagnetic torque(T_e), produced by DFIG is expressed by

$$T_e = \frac{1}{2} X_m ((i_{qs} + i_{qr}) i_{dr} + (i_{qs} + i_{qr}) i_{qr}). \tag{15}$$

Where, X_m is the magnetizing reactance of the induction generator. Since the study system is found unstable at 75% compensation level and 90% compensation level, at 7 m/sec wind speed, these two cases are considered for assessment. In both cases, R is kept 1 and the weighted matrix Q for 75% and 90% compensation are as below

$$Q_{75} = \begin{bmatrix} 0.2526 & 0 & 0 & 0 \\ 0 & 0.7289 & 0 & 0 \\ 0 & 0 & 1.969\times10^{-7} & 0 \\ 0 & 0 & 0 & 0.6965 \end{bmatrix} \tag{16}$$

$$Q_{90} = \begin{bmatrix} 0.2440 & 0 & 0 & 0 \\ 0 & 0.7350 & 0 & 0 \\ 0 & 0 & 8.5392\times10^{-5} & 0 \\ 0 & 0 & 0 & 0.6929 \end{bmatrix} \tag{17}$$

Here off-diagonal elements are penalty factors for state variables associated with T_e.

III. RESULTS AND DISCUSSION

In the previous section LQR method is discussed for the calculation of Q and R weighted matrices in order to reduce the error in electromagnetic torque (T_e) signal. Hence this section elaborates on the efficacy of LQR with SSSC for SSR mode dampening through eigenvalue analysis and time domain simulations. In Section 2, the analysis of SSR stability at different wind speeds and compensation levels is shown, and critical conditions which can lead the system to instability were investigated through eigenvalue analysis.

Eigenvalue Analysis. This section shows the analysis of the eigenvalues computed to verify the efficacy of the proposed approach. The comparison of the list of eigenvalues for important modes is discussed, which is shown in Table 4 and 5. These tables include a list of eigenvalues for only SSSC and SSSC with the LQR approach for 75% and 90% compensation levels, respectively. With the LQR approach, both tables shows significant improvement in the stability of SSR mode. For 75%, compensation level damping of SSR mode is increased from 6.58%to 50.49%, and for 90%, compensation level damping of SSR mode is increased from 1.028% to 8.68%. Table 3 and Table 4 shows that with low wind speed (7 m/s) and high compensation level (75% and 90%) sub-synchronous mode and super-synchronous mode are stable. In both compensation level cases along with SSR mode, shaft mode, electromechanical mode, and torsional modes are also found stable in both compensation level cases after inclusion of LQR approach. The results exhibit the significant increment in damping ratio of all important modes too.

Eigenvalue plot for study system, study system after adding SSSC controller and study system with LQR approach for both compensation level cases are shown in Fig. 4 and 5. In both cases, SSR mode has shifted significantly left side of s-plane at new poles as listed in Table 3 and Table 4.

Table 3: Lists of Eigenvalues for 75% Compensation Levels and 7 m/s wind speed.

Mode	75% Compensation Level			
	Without LQR control		With LQR control	
	$\sigma \pm i\omega$	$\delta(\%)$	$\sigma \pm i\omega$	$\delta(\%)$
Super-synchronous	-12.344 ± 556.39i	2.21%	-68.9616±539.08i	12.68%
Sub-synchronous	-5.030 ± 138.23i	3.65%	-84.8478±145.02i	50.49%
Shaft	0.48842 ± 6.1493i	7.91%	-0.4970 ± 6.1465i	8.06%
Torsional	-85.883 ± 37.936i	91.47%	-88.9875 ± 38.14i	91.91%
Electromechanical	-9.6224 ± 94.729i	10.10%	-4.5571 ± 93.6414i	4.56%

Table 4: Lists of Eigenvalues for 90% Compensation Levels and 7 m/s wind speed.

Mode	90% Compensation Level			
	Without LQR control		With LQR control	
	$\sigma \pm i\omega$	$\delta(\%)$	$\sigma \pm i\omega$	$\delta(\%)$
Super-synchronous	-13.605 ± 570.94i	2.38%	-68.831±555.83i	12.28%
Sub-synchronous	-2.2401 ± 114.64i	1.02%	-82.964±115.06i	58.48%
Shaft	-0.48455 ± 6.1504i	7.85%	-0.4987 ± 6.1483i	8.08%
Torsional	-86.534 ± 37.766i	91.65%	-90.40 ± 38.8064i	91.89%
Electromechanical	-19.362 ± 91.845i	20.62%	-4.76 ± 93.5226i	5.06%

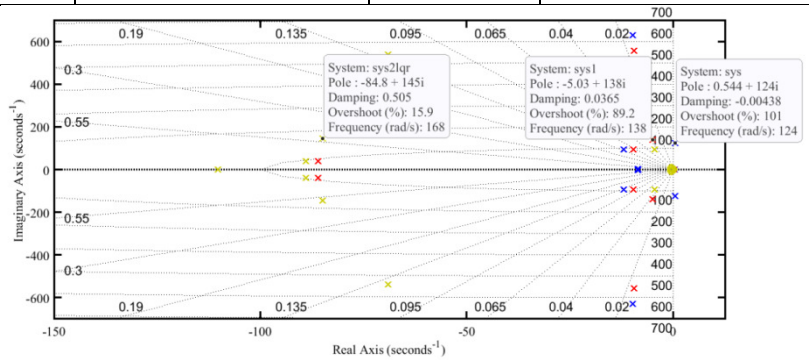

Fig. 4. Comparison of Eigenvalues for 75% compensation level at 7 m/s wind speed.

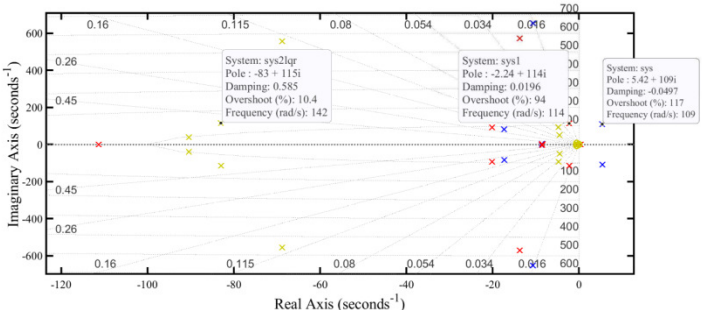

Fig. 5. Comparison of Eigenvalues for 90% compensation level at 7 m/s wind speed.

Time Domain Analysis. In this section, time domain results obtained through transient simulation of a combined study system without SSSC, with SSSC, and with SSSC added with LQR are discussed. For transient simulation, MATLAB-SIMULINK is used. A study discussed in Section 2 shows that when wind speed is low (7 m/s) and compensation level is high (75% and above), the system suffers SSR instability due to IGE. The effectiveness of SSSC for SSR alleviation is studied with two scenarios:

1. Wind speed is 7 m/s and compensation level is 75%,
2. Wind speed is 7 m/s and the compensation level is 90%.

The initial values of state variables of the study system are computed through equilibrium conditions where all derivative terms are assumed to be zero.

A. Scenario 1

Fig. 6 shows a comparison of dynamic responses of the study system with above mentioned three cases when wind speed is 7 m/s and compensation level is 75%. The red line denotes the system added with SSSC, the blue line denotes the system without SSSC and the green line shows the study system's response with LQR and SSSC. It is seen that the system without SSSC is unstable due to large oscillations when the compensation level is 75%. In comparison, the response of the study system with only SSSC shows transients in the initial period. Response of study system after adding LQR approach shows further significant improvement in mitigating SSR oscillation. Fig. 6 shows dynamic responses of electromagnetic torque T_e, rms current through transmission line il and voltage across series capacitor v_c rotor speed of induction generator ω_r. Waveforms shown in both figures verify the eigenvalue stability results.

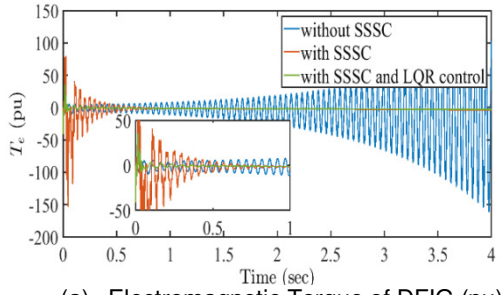

(a) Electromagnetic Torque of DFIG (pu).

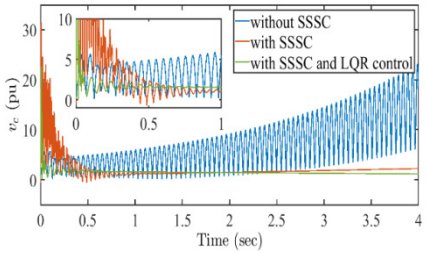

(b) RMS voltage across FSC (pu)

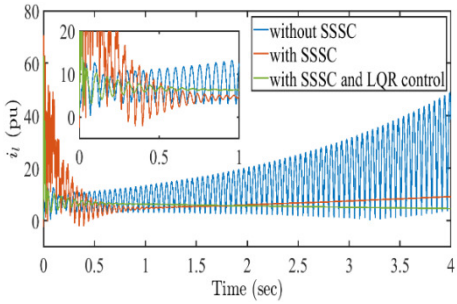

(c) RMS current through transmission line (pu).

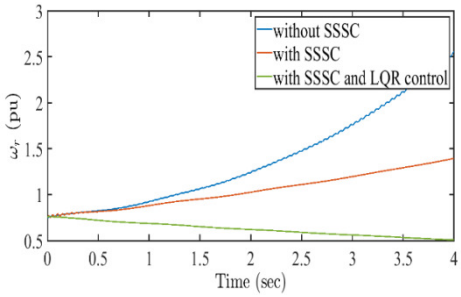

(d) Rotor speed of DFIG (pu)

Fig. 6. Dynamic responses of study system variables for different approaches for 75% comp. level and 7 m/s wind speed.

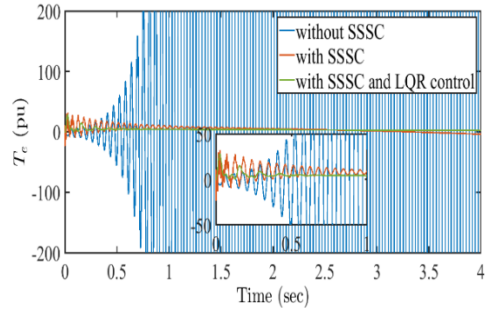

(a) Electromagnetic Torque of DFIG (pu)

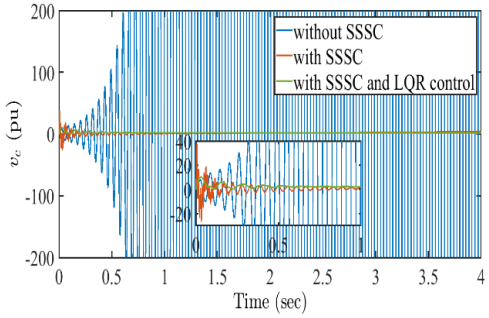

(b) RMS voltage across FSC (pu)

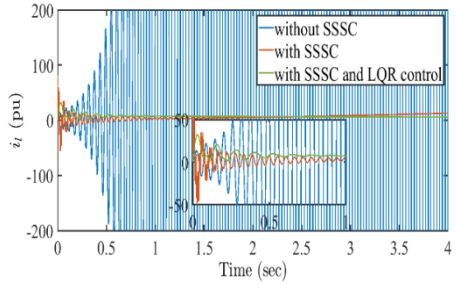

(c) RMS current through transmission line (pu)

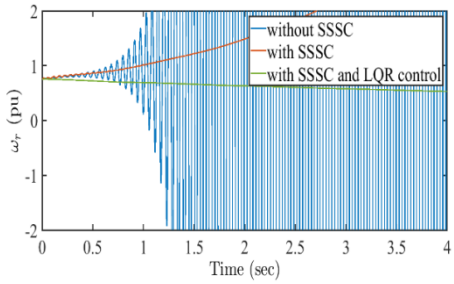

(d) Rotor speed of DFIG (pu)

Fig. 7. Dynamic responses of study system variables for different approaches for 90% comp. Level and 7 m/s wind speed.

B. Scenario 2

In this scenario compensation level is 90% with 7 m/s wind speed and transient responses of discussed study system are shown in Fig. 7. It is seen that initially transient report is observed up to few milliseconds and then waveforms have followed to stable value for new operating condition obtained after adding SSSC. But the response of study system with SSSC along with LQR waveforms shows highest improved stability. The magnitude of oscillation has reduced significantly. This proves that LQR provides positive damping torque. In both scenarios, results obtained through time-domain simulations corroborate the eigenvalue analysis discussed in the previous section. Thus, SSR is observed in unstable conditions at higher compensation levels, and the light wind is further significantly damped through the SSR damping controller with LQR, as shown in the above time domain results.

IV. CONCLUSION

This paper presents the design procedure and ability of LQR with SSSC for the enhancement of SSR alleviation. The LQR-based damping control scheme for the DFIG-based series compensated network minimizes the error of electromagnetic torque of DFIG as it reflects SSR instability superiorly. To alleviate SSR oscillations,

the LQR controls the voltage injected by SSSC in order to modulate the torque signal. Since the response of DFIG torque depends on stator and rotor currents, the effectiveness of the proposed approach is shown by choosing the weight matrices to damp SSR oscillation quickly. The eigenvalue results show that LQR shifts and detunes SSR mode and damping ratio has increased significantly. Time domain results also verify the proposed approach's effectiveness by exhibiting the damped and stable response of the study system after incorporating LQR control.

FUTURE SCOPE

This paper shows the efficacy of LQR based mitigation approach with SSSC to mitigate SSR by regulating the electromagnetic torque signal of DFIG and modulating the SSSC output. Furthermore, there are different signals that exhibit the SSR instability such as line current, fixed series capacitor voltage, DFIG terminal voltage, and rotor speed. Such signals can also be regulated to dampen the abrupt SSR oscillations.

Acknowledgment. We would like to acknowledge the support and sources provided by our family and Sardar Vallabhbhai National Institute of Technology, Surat, as a part of the encouragement to allow us to do the research work presented in this paper.
Conflict of Interest. No conflict of interest

REFERENCES

[1]. Brinkman, G. (2021). The North American Renewable Integration Study: a US Perspective. National Renewable Energy Laboratory.
[2]. Erlich, I., Shewarega, F., Feltes, C., Koch, F. W., & Fortmann, J. (2013). Offshore wind power generation technologies. *Proceedings of the IEEE, 101*(4), 891-905.
[3]. Jiang, Z., Zhu, X., & Hu, W. (2018). Modeling and analysis of offshore floating wind turbines. In *Advanced Wind Turbine Technology* (pp. 247-280). Springer, Cham.
[4]. Wang, L., Wei, J., Wang, X., & Zhang, X. (2009). The development and prospect of offshore wind power technology in the world. In *2009 World Non-Grid-Connected Wind Power and Energy Conference* (pp. 1-4). IEEE.
[5]. Luo, L., Cheng, X., Zong, X., Wei, W., & Wang, C. (2015, August). Research on transmission line loss and carrying current based on temperature power flow model. In 2015 3rd International Conference on Mechanical Engineering and Intelligent Systems (pp. 120-127). Atlantis Press.
[6]. Luo, L., Cheng, X., Zong, X., Wei, W., & Wang, C. (2015). Research on transmission line loss and carrying current based on temperature power flow model. In *2015 3rd International Conference on Mechanical Engineering and Intelligent Systems* (pp. 120-127). Atlantis Press.
[7]. Nurdin, M., Hariyanto, N., Sasmono, S., Rahmani, R., & Faizal, R. (2012, September). Fix series capacitor for increasing power transfer on transmission 150 kV at Sumatera interconection system. In *2012 IEEE International Conference on Condition Monitoring and Diagnosis* (pp. 565-568). IEEE.
[8]. Mohammadpour, H. A., Islam, M. M., Santi, E., & Shin, Y. J. (2015). SSR damping in fixed-speed wind farms using series FACTS controllers. *IEEE Transactions on Power Delivery*, *31*(1), 76-86.
[9]. Mohammadpour, H. A., & Santi, E. (2015). Analysis of subsynchronous control interactions in DFIG-based wind farms: ERCOT case study. In *2015 IEEE Energy Conversion Congress and Exposition (ECCE)* (pp. 500-505). IEEE.
[10]. Rohit, C. V., Darji, P. B., & Jariwala, H. R. (2018). Mitigation of IGE using STATCOM with DFIGs. In *2018 IEEE International Conference on Power Electronics, Drives and Energy Systems (PEDES)* (pp. 1-6). IEEE.
[11]. Rohit, C., Darji, P. B., & Jariwala, H. R. (2021). A Stability Assessment and Estimation of Equivalent Damping Gain for SSR Stability by Nyquist stability criterion in DFIG-based windfarms. In *2021 31st Australasian Universities Power Engineering Conference (AUPEC)* (pp. 1-6). IEEE.
[12]. Miao, Z. (2012). Impedance-model-based SSR analysis for type 3 wind generator and series-compensated network. *IEEE Transactions on Energy Conversion*, *27*(4), 984-991.
[13]. Wang, L., Liang, H. R., Prokhorov, A. V., Mokhlis, H., & Huat, C. K. (2019). Modal control design of damping controllers for thyristor-controlled series capacitor to stabilize common-mode torsional oscillations of a series-capacitor compensated power system. *IEEE Transactions on Industry Applications*, *55*(3), 2327-2336.
[14]. Edris, A. A. (1990). Series compensation schemes reducing the potential of subsynchronous resonance. *IEEE transactions on power systems*, *5*(1), 219-226.
[15]. Abdeen, M., Emran, A., Moustafa, A., Kamal, D., Hassan, R., Hassan, E., & Jurado, F. (2021). Investigation on TCSC Parameters and Control Structure for SSR Damping in DFIG-Based Wind Farm. In *2021 12th International Renewable Energy Congress (IREC)* (pp. 1-5). IEEE.
[16]. Leon, A. E. (2015). Integration of DFIG-based wind farms into series-compensated transmission systems. *IEEE Transactions on Sustainable Energy*, *7*(2), 451-460.
[17]. Fan, L., Kavasseri, R., Miao, Z. L., & Zhu, C. (2010). Modeling of DFIG-based wind farms for SSR analysis. *IEEE Transactions on Power Delivery*, *25*(4), 2073-2082.
[18]. Mahalakshmi, R., & Thampatty, K. C. (2020). Design and implementation of modified RSC controller for the extenuation of sub-synchronous resonance oscillations in series compensated DFIG-based WECS. *International Transactions on Electrical Energy Systems*, *30*(7).
[19]. Huang, P. H., El Moursi, M. S., Xiao, W., & Kirtley, J. L. (2014). Subsynchronous resonance mitigation for series-compensated DFIG-based wind farm by using two-degree-of-freedom control strategy. *IEEE Transactions on Power Systems*, *30*(3), 1442-1454.
[20]. Leon, A. E., & Solsona, J. A. (2014). Sub-synchronous interaction damping control for DFIG wind turbines. *IEEE Transactions on Power Systems*, *30*(1), 419-428.
[21]. Xie, X., Zhang, X., Liu, H., Liu, H., Li, Y., & Zhang, C. (2017). Characteristic analysis of subsynchronous resonance in practical wind farms connected to series-compensated transmissions. *IEEE Transactions on Energy Conversion*, *32*(3), 1117-1126.

[22]. Liu, H., Xie, X., Zhang, C., Li, Y., Liu, H., & Hu, Y. (2016). Quantitative SSR analysis of series-compensated DFIG-based wind farms using aggregated RLC circuit model. *IEEE Transactions on Power Systems, 32*(1), 474-483.
[23]. Varma, R. K., Axente, I., & Litzenberger, W. H. (2010, July). Bibliography of FACTS: 2006–2007 Part I IEEE working group report. In *IEEE PES General Meeting* (pp. 1-6). IEEE.
[24]. Padiyar, K. R., & Varma, R. K. (1991). Damping torque analysis of static var system controllers. *IEEE Transactions on Power Systems*, *6*(2), 458-465.
[25]. Varma, R. K., & Auddy, S. (2006). Mitigation of subsynchronous oscillations in a series compensated wind farm with static var compensator. In *2006 IEEE Power Engineering Society General Meeting* (pp. 7-pp). IEEE.
[26]. Piyasinghe, L., Miao, Z., Khazaei, J., & Fan, L. (2014). Impedance model-based SSR analysis for TCSC compensated type-3 wind energy delivery systems. *IEEE Transactions on Sustainable Energy*, *6*(1), 179-187.
[27]. Chernet, S. (2018). *Subsynchronous Resonance in Doubly Fed Induction Generator Based Wind Farms*. Chalmers Tekniska Hogskola (Sweden).
[28]. Mohammadpour, H. A., & Santi, E. (2014). Modeling and control of gate-controlled series capacitor interfaced with a DFIG-based wind farm. *IEEE Transactions on Industrial Electronics*, *62*(2), 1022-1033.
[29]. Mohammadpour, H. A., & Santi, E. (2014, September). Sub-synchronous resonance analysis in DFIG-based wind farms: Mitigation methods—TCSC, GCSC, and DFIG controllers—Part II. In *2014 IEEE energy conversion congress and exposition (ECCE)* (pp. 1550-1557). IEEE.
[30]. Olalla, C., Leyva, R., El Aroudi, A., & Queinnec, I. (2009). Robust LQR control for PWM converters: An LMI approach. *IEEE Transactions on industrial electronics*, *56*(7), 2548-2558.
[31]. Rohit, C., Darji, P., & Jariwala, H. (2022). Modelling and control of static synchronous series compensator interfaced with DFIG-based wind farm using PSO for SSR alleviation. *International Journal of Ambient Energy*, 1-14.
[32]. Abhinav, S., & Pal, B. C. (2018). *Dynamic estimation and control of power systems*. Academic Press.
[33]. Ewais, A. M., Liang, J., Ekanayake, J. B., & Jenkins, N. (2012). Influence of Fully Rated Converter-based wind turbines on SSR. In *IEEE PES Innovative Smart Grid Technologies* (pp. 1-6). IEEE.
[34]. Ghafouri, M., Karaagac, U., Karimi, H., Jensen, S., Mahseredjian, J., & Faried, S. O. (2017). An LQR controller for damping of subsynchronous interaction in DFIG-based wind farms. *IEEE Transactions on Power Systems*, *32*(6), 4934-4942.

How to cite this article: Chirag Rohit, Pranav B. Darji and Hitesh R. Jariwala (2022). Linear-Quadratic Regulator-based SSR Mitigation Scheme for SSSC Controller in DFIG-based SERIES Compensated Network. *International Journal on Emerging Technologies, 13*(1): 56–64.